

## Oxygen Species Formed on Different Surface Sites of CaO by Decomposition of N<sub>2</sub>O and the Reactivity

MASATO NAKAMURA, HIROYUKI MITSUHASHI, AND NOBUTSUNE TAKEZAWA

*Department of Chemical Process Engineering, Hokkaido University, Sapporo 060, Japan*

Received March 25, 1992; revised June 25, 1992

Adsorbed oxygen species were appreciably formed on CaO by decomposition of N<sub>2</sub>O. By temperature programmed desorption the activation energy of the desorption of oxygen was estimated to be 44–45 kcal/mol at amounts of adsorption below 0.15  $\mu\text{mol}/\text{m}^2\text{CaO}$ . It decreased rapidly with increased amounts of adsorbed oxygen species, staying at 31 kcal/mol above 0.5  $\mu\text{mol}/\text{m}^2\text{CaO}$ . Photoluminescence spectra of CaO suggested that adsorbed oxygen species were preferentially held on surface sites with low coordination number (coordination number of 4) at small amounts of adsorption whereas at large amounts of adsorption adsorbed oxygen species were mostly held on surface sites with high coordination number (coordination number of 5). The oxygen species formed on the former sites were more active than those formed on the latter sites for the oxidative dehydrogenation of ethane. Ethene was produced with high selectivity. © 1992 Academic Press, Inc.

### INTRODUCTION

It has been prevailingly accepted that molecular oxygen is sparingly chemisorbed on alkaline earth metal oxides unless the oxides are exposed to neutrons,  $\gamma$  rays, or ultraviolet rays (1–7). However, in the course of the decomposition of N<sub>2</sub>O adsorbed oxygen species were appreciably produced on CaO (8).

In the present work, we show that by temperature programmed desorption and temperature programmed reaction methods and photoluminescence spectroscopy oxygen species formed on surface sites of CaO with low coordination number were strongly held on the surface and were highly effective for the oxidative dehydrogenation of ethane as compared with those formed on surface sites with high coordination number.

### EXPERIMENTAL

CaO (0.76 g) was prepared by decomposition of calcium carbonate (Nakarai Chemicals Ltd., extra pure grade) at 1073 K for 2 h in vacuum. The N<sub>2</sub>O decomposition was carried out in a conventional flow reactor at a total flow rate of 150 cm<sup>3</sup> NTP/min (hence-

forth described in cm<sup>3</sup>). Temperature programmed desorption (TPD) of oxygen was carried out in a helium stream of 30 cm<sup>3</sup>/min at heating rates of 2–24 K/min to a temperature of 1073 K. Temperature programmed reaction (TPRx) was carried out with ethane at a heating rate of 7 K/min to a temperature of 923 K. The partial pressure of ethane in the inflow was always kept at 0.1 atm. The total flow rate was kept at 30 cm<sup>3</sup>/min.

The reactants and the products were analyzed by a gas chromatograph (Hitachi 163) with thermal conductivity and flame ionization detectors. In the TPD and TPRx runs, gases from the reactor were collected every 3 min in sampling tubes attached to the outlet of the reactor for analysis and admitted to the gas chromatograph. O<sub>2</sub>, N<sub>2</sub>, and H<sub>2</sub> in the effluent were separated by a column packed with molecular sieve 5A whereas C<sub>2</sub>H<sub>4</sub>, C<sub>2</sub>H<sub>6</sub>, and CO<sub>2</sub> were separated by a column packed with Porapak Q. Except for analysis of H<sub>2</sub>, helium was used as the carrier gas. For analysis of H<sub>2</sub>, nitrogen was used as the carrier gas. Photoluminescence spectra of the catalysts were obtained in vacuum at 298 K on a fluorescence spectrophotometer (Hitachi 650-S). The BET sur-

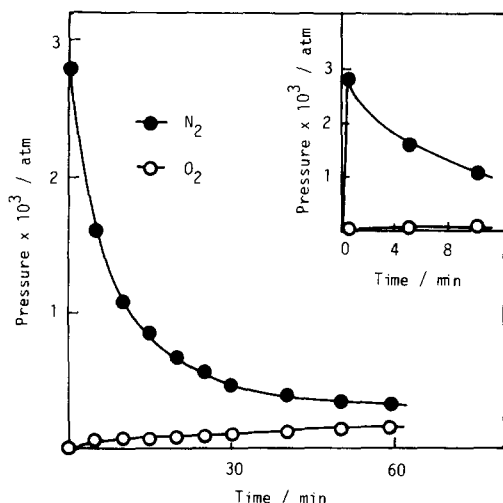


FIG. 1. Partial pressures of nitrogen and oxygen in the effluent under transient state of the  $\text{N}_2\text{O}$  decomposition over CaO. The decomposition was carried out at 573 K. The inset shows the partial pressures of nitrogen and oxygen at the initial period of the transient state.

face area of CaO was estimated to be  $33.5 \text{ m}^2/\text{g}$  by the adsorption of nitrogen at 77 K.

## RESULTS AND DISCUSSION

### Temperature Programmed Desorption of Adsorbed Oxygen Species

When  $\text{N}_2\text{O}$  was fed over CaO, the decomposition  $\text{N}_2\text{O} \rightarrow \text{N}_2 + \frac{1}{2} \text{O}_2$  occurred above 473 K. Figure 1 illustrates the partial pressures of nitrogen and oxygen in the effluent as functions of the reaction time at 573 K. Partial pressure of nitrogen in the effluent overshoots rapidly and then decreases to a steady state value, whereas that of oxygen grows to a steady state value in a monotonic manner. Under the present experimental conditions, the conversion of  $\text{N}_2\text{O}$  was always lower than 3%. Hence, the partial pressure of  $\text{N}_2\text{O}$  was practically constant throughout the catalyst bed. Under the transient state of the reaction the partial pressure of nitrogen exceeded greatly that of oxygen expected from the stoichiometry of the decomposition reaction. This strongly suggests that adsorbed oxygen species are

appreciably formed on CaO in the course of the decomposition of  $\text{N}_2\text{O}$ .

Figure 2 illustrates TPD profiles of adsorbed oxygen species formed by the decomposition of  $\text{N}_2\text{O}$  at 573 K for various periods of time. A strong peak of oxygen desorption occurs at 643–740 K. No other species were evolved in the course of the TPD runs, suggesting that nitrogen-containing species were absent on the surface. The intensity of the desorption peak of oxygen increases with increased reaction time. Unless  $\text{N}_2\text{O}$  was previously decomposed, no desorption occurred. After exposure to a stream of  $\text{N}_2\text{O}$  at 573 K for 1 h, oxygen desorbed amounted to as much as  $2.9 \mu\text{mol}/\text{m}^2 \text{ CaO}$ . On the basis of the BET surface area of the present sample, this corresponds to 27 or 54% of the surface  $\text{Ca(II)}$  sites, assuming molecular or atomic adsorption. In great contrast to these observations, over the catalyst exposed to molecular oxygen at 573 K, no oxygen was desorbed.

In Fig. 3, the total amount of oxygen de-

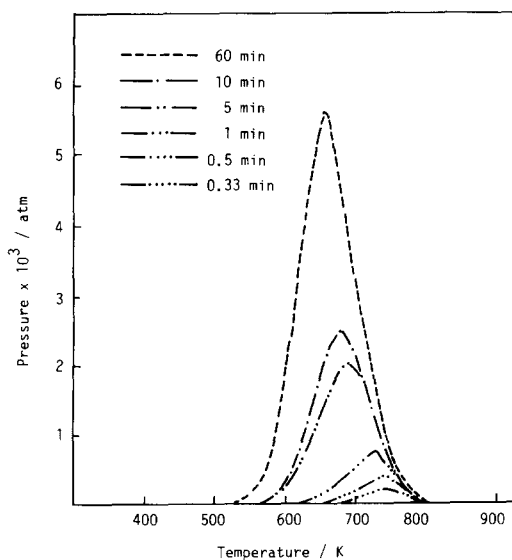


FIG. 2. TPD profiles of oxygen formed by the decomposition of  $\text{N}_2\text{O}$ . The decomposition was carried out at 573 K for various periods of time. Numbers represented in min in the figure show the reaction time.

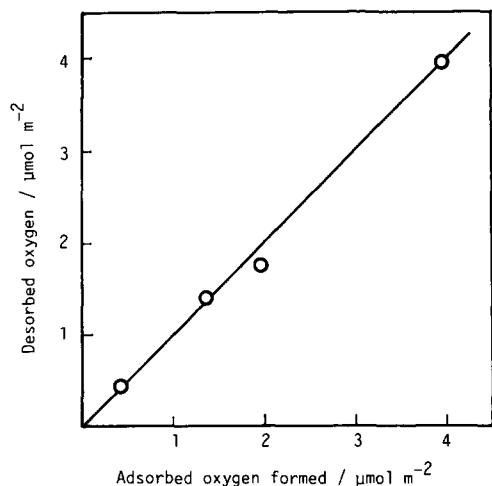


FIG. 3. Amount of adsorbed oxygen species in TPD runs versus amount of adsorbed oxygen species formed under the transient state of the decomposition of  $N_2O$ . The decomposition was carried out at 573 K.

sorbed in TPD runs is plotted against that formed in the decomposition of  $N_2O$ . The former value is in good accord with the latter value, strongly suggesting that all adsorbed oxygen species formed in the decomposition of  $N_2O$  are desorbed in the TPD runs.

The activation energy of the desorption and the desorption order can be determined on the basis of TPD profiles obtained. On the assumption that the reactor behaves as a continuously stirred tank reactor, the mass balance of oxygen in TPD runs yields the equation

$$fV \frac{dP}{dt} = r - vP, \quad (1)$$

where  $f$ ,  $V$ ,  $P$ ,  $t$ ,  $r$ , and  $v$  represent the void fraction of the catalyst bed, the volume of the catalyst bed, the partial pressure of oxygen in the effluent, time, the rate of the oxygen desorption, and the total flow rate, respectively. Since the desorption was conducted in a linear temperature rise with respect to time as

$$T = T_0 + gt, \quad (2)$$

where  $T$  is the temperature,  $T_0$  is the temper-

ature at which TPD runs start, and  $g$  is a coefficient of temperature rise, we can re-write Eq. (1) as

$$r = vP + (gfV) \frac{dP}{dT}. \quad (3)$$

Under the present experimental conditions, the term  $(gfV)dP/dT$  is always smaller than 0.5% of  $vP$ . Hence, Eq. (3) can be rewritten as

$$r = vP. \quad (4)$$

We can estimate the amount of adsorbed oxygen species,  $N$ , present at a given temperature,  $T$ , of a TPR run by integration of a TPD curve as

$$N = (v/g) \int_T^{T_f} P dT, \quad (5)$$

where  $T_f$  is the temperature at which  $P$  reaches 0 above  $T$ . From TPD curves obtained at various heating rates or those for various amount of oxygen species, we can determine  $P$ - and  $N$ -values at a given temperature. Hence, we can estimate the rate of the desorption of oxygen as a function of  $N$  at a given temperature by using Eqs. (4) and (5).

In Fig. 4,  $\log r$  is plotted against  $\log N$ . A good linear relationship exists between these parameters. The rate of the desorption,  $r$ , is approximated to be the second order in the amount of adsorbed oxygen species. From the plot in this figure,  $r$ -values at a given  $N$  can be obtained at various temperatures. A good linear relationship existed between  $\ln r$  and  $1/T$ . From the slope of the straight line thus obtained, the activation energy of the desorption of oxygen were estimated.

Figure 5 shows how the activation energy varies with the amount of adsorbed oxygen species. At small amounts of adsorption the activation energy approaches 44–45 kcal/mol. It decreases rapidly above 0.15  $\mu\text{mol}/\text{m}^2$  CaO of adsorbed oxygen species and stays at 31 kcal/mole above 0.5  $\mu\text{mol}/\text{m}^2$

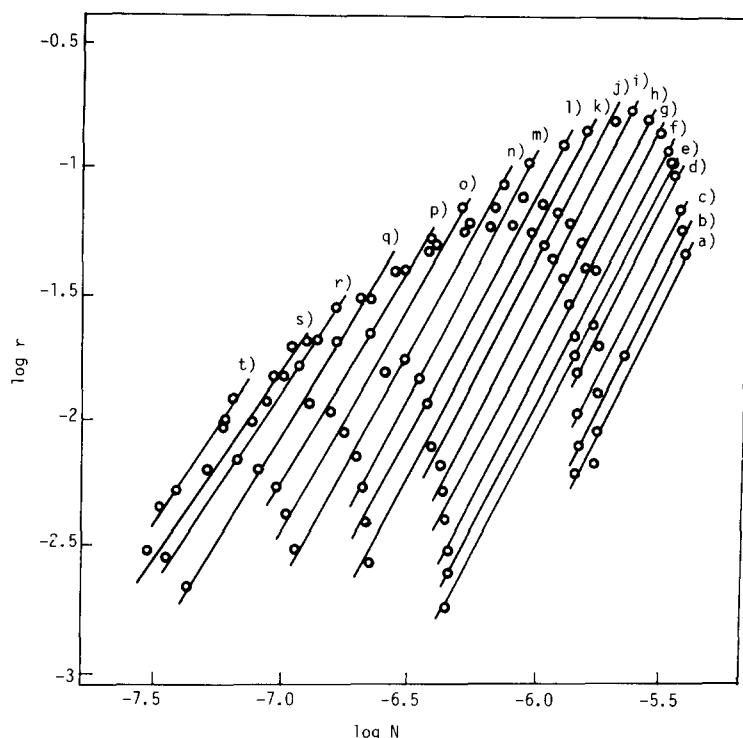


FIG. 4. Relationship between  $\log r$  and  $\log N$ . Temperature (in K), (a) 593, (b) 598, (c) 603, (d) 613, (e) 618, (f) 623, (g) 633, (h) 643, (i) 653, (j) 663, (k) 673, (l) 683, (m) 693, (n) 703, (o) 713, (p) 723, (q) 733, (r) 743, (s) 753, (t) 763.

CaO. This strongly suggests that the surface sites for adsorbed oxygen species are non-homogeneous.

#### *Effect of Adsorbed Oxygen Species upon the Photoluminescence Spectra of CaO*

Figure 6 illustrates the photoluminescence spectra of CaO. A peak occurs at 298 nm in the excitation spectrum whereas one occurs at 400 nm in the emission spectrum. According to Garrone *et al.* (9) and Collucia *et al.* (10), these peaks are ascribable to the sites with a coordination number of 4. On the basis of ultraviolet diffuse reflectance spectra of CaO observed by Zecchina *et al.* (11), Garrone *et al.* (9) concluded that an excitation peak occurred around 340 nm for sites with a coordination number of 3. Since no distinct peak was discerned around this region in the present spectra, the number of these sites would be practically negligible compared with the number of sites with a

coordination number of 4. Garrone *et al.* (9) and Collucia *et al.* (10) also showed that the sites with a coordination number of 5, i.e., the sites on (100) faces of CaO, gave an excitation peak at wavenumber below 230 nm on the basis of the Levine-Mark theory

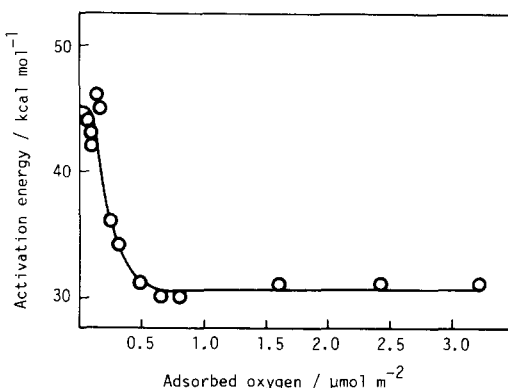


FIG. 5. Activation energy of the desorption of oxygen versus amount of adsorbed oxygen species.

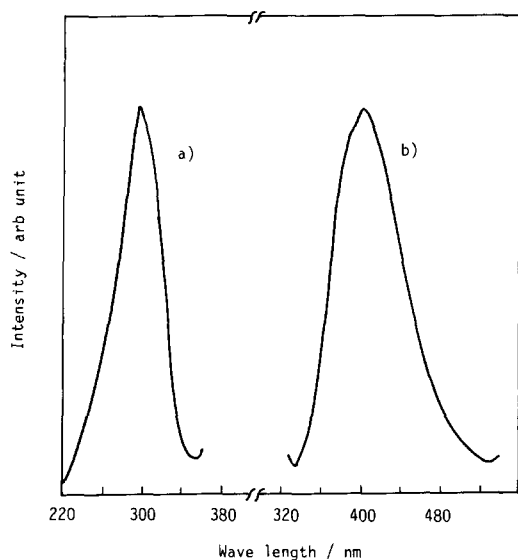


FIG. 6. Photoluminescence spectra of CaO at 298 K: (a) excitation spectrum of 400 nm luminescence, (b) emission excited at 298 nm.

(12). However, no peak is seen in the wave length region at 220–230 nm in the present spectra. The peak probably lay beyond the wavelength range where we measured the spectra.

Photoluminescence spectra were obtained for the catalyst with various amounts of adsorbed oxygen species. The intensities of the peaks at 298 and 400 nm were found to decrease markedly with increased amounts of adsorbed oxygen species. The positions of the peaks remained practically unchanged.

Figure 7 shows how the intensity of the emission peak varies with the presence of adsorbed oxygen species. Over catalysts having  $0.15 \mu\text{mol}/\text{m}^2\text{CaO}$  of adsorbed oxygen species, the intensity decreases by 90%. This strongly suggests that the oxygen species were preferentially held on the sites with a coordination number of 4 below  $0.15 \mu\text{mol}/\text{m}^2\text{CaO}$  of adsorbed oxygen species. At the amount of adsorbed oxygen species rises above  $0.15 \mu\text{mol}/\text{m}^2\text{CaO}$ , the other surface sites should be responsible for the formation of the oxygen species. As described

above, in the decomposition of  $\text{N}_2\text{O}$  for 1 h the amount of adsorbed oxygen species formed was estimated to be as much as 27 or 54% of the surface for the molecular or atomic adsorption. Hence, the rest of the adsorbed oxygen species were most likely held on the sites abundantly present on the surface. According to electron microscopic observations by Garrone *et al.* (9), Collucia and Tench (13), and Kikuchi and co-workers (14), (100) faces were preferentially exposed on the surfaces of MgO particles prepared from magnesium hydroxide, magnesium carbonate, or basic magnesium carbonate. Thus, the present CaO sample would have surface structures similar to those of MgO. On these grounds, we concluded that sites with a coordination number of 5 were abundantly present on the surface and were involved in the formation of adsorbed oxygen species. On the basis of the surface area of the present sample, we can estimate the average size of CaO particles (assumed to exhibit cubic structures) to be 54.3 nm. Hence, the number of surface sites on edges of the CaO cubes was estimated to

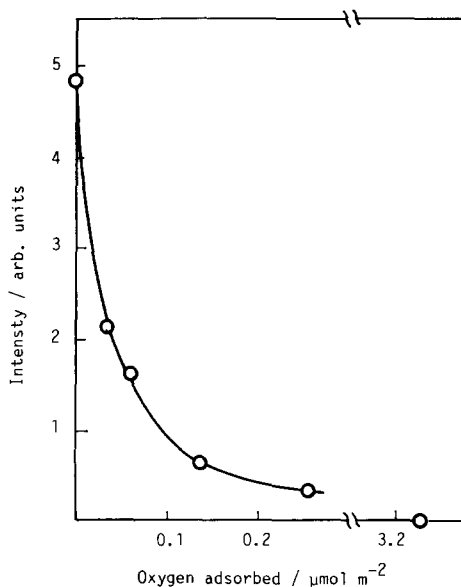


FIG. 7. Intensity of the emission peak at 400 nm against the amount of adsorbed oxygen species.

be about 1% of the total number of the surface sites on the present sample, corresponding to  $0.07\text{--}0.14 \mu\text{mol}/\text{m}^2\text{CaO}$  for atomically or molecularly adsorbed oxygen species at saturation of the edge sites. This estimated value was in fair agreement with the critical amount of adsorbed oxygen species at which the intensity of the photoluminescence peaks decreased considerably. Hence, we concluded that the edge sites were primarily responsible for the formation of adsorbed oxygen species at small amount of the adsorption.

#### States of the Adsorbed Oxygen Species

In recent work using IR spectroscopy (15), we found that absorption occurred at  $880 \text{ cm}^{-1}$  for CaO exposed to the decomposition of  $\text{N}_2\text{O}$ . With the help of temperature programmed decomposition of  $\text{CaO}_2$  and the hydrolysis of adsorbed oxygen species, we concluded that a considerable amount of peroxide species in a side-on structure



was formed by the decomposition of  $\text{N}_2\text{O}$ . The decomposition of metal peroxides was suggested to be a bimolecular reaction (6, 16, 17). Hence, the second order kinetics found in the present experiments can also be consistently ascribed to the decomposition of surface peroxide species formed on CaO. Because of the side-on structure of the surface peroxide species, Ca(II) sites on edges of CaO cubes would be sterically more favorable for the formation of these species than those on (100) faces. Hence, it is highly probable that surface peroxide species are strongly held on the Ca(II) sites with coordination number 4 as compared with those with coordination number 5.

#### Temperature Programmed Desorption of Ethane with Adsorbed Oxygen Species

Figure 8 shows TPRx profiles of ethane. In the absence of adsorbed oxygen species, a broad peak of ethene formation is observed at  $550\text{--}700 \text{ K}$ . Above  $720 \text{ K}$  the ethene for-

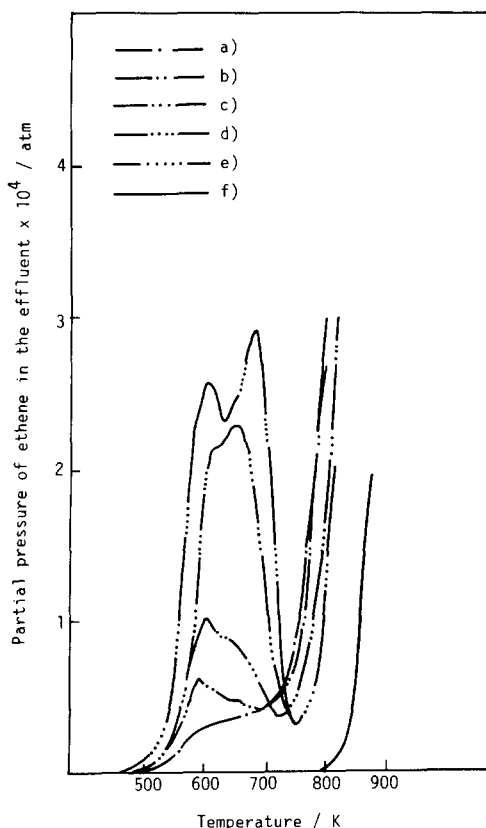


FIG. 8. Partial pressure of ethane in the effluent in the course of TPRx runs with ethane. Adsorbed oxygen species were previously formed by the decomposition of  $\text{N}_2\text{O}$ . TPRx runs were conducted over catalysts with various amounts (in  $\mu\text{mol}/\text{m}^2\text{CaO}$ ) of adsorbed oxygen species. The amounts of the oxygen species (in  $\mu\text{mol}/\text{m}^2\text{CaO}$ ) are (a) 0, (b) 0.013, (c) 0.048, (d) 0.16, and (e) 0.37. The TPRx profile represented in (f) was obtained in an empty reactor.

mation increases markedly with increased temperature. During the course of the TPRx runs, neither carbon dioxide nor carbon monoxide was detected in the effluent. In separate experiments, hydrogen was detected in the effluent above  $720 \text{ K}$ . Under these conditions, the partial pressure of hydrogen in the effluent was practically the same as that of ethene. This suggests that the dehydrogenation of ethane,  $\text{C}_2\text{H}_6 \rightarrow \text{C}_2\text{H}_4 + \text{H}_2$ , occurred selectively. When ethane is fed through an empty reactor, the dehydrogenation takes place slowly as com-

pared with that over CaO. The formation of ethene is appreciable above 800 K. The dehydrogenation of ethane was accelerated by the presence of CaO.

In the presence of adsorbed oxygen species, the formation of ethene begins at a lower temperature, 470 K. Two peaks of the ethene formation are observed at 600 and 670 K (referred to as  $\alpha$ - and  $\beta$ -peak, respectively). Above 720–740 K, the formation of ethene increases with increased temperature. At small amounts of adsorbed oxygen species,  $\alpha$ -peak appears in preference to  $\beta$ -peak. As the amount of adsorbed oxygen species increases,  $\beta$ -peak grows more rapidly than  $\alpha$ -peak. No oxygen was desorbed throughout TPRx runs. Hydrogen was desorbed above 720–740 K. These findings strongly suggested that ethene was produced by the oxidative dehydrogenation of ethane with adsorbed oxygen species below 720–740 K whereas above 720–740 K ethene was produced by the dehydrogenation of ethane. It is highly probable that  $\alpha$ -peak resulted from the reaction of ethane with oxygen species located at the surface sites of a coordination number of 4 whereas  $\beta$ -peak resulted from that of ethane with oxygen species located at the surface sites of a coordination number of 5. Oxygen species located at the former sites were more active for oxidative dehydrogenation to ethene than at the latter sites.

During the course of the TPRx runs, carbon dioxide and carbon monoxide were undetected in the effluent. After the catalyst was subjected to TPRx of ethane with adsorbed oxygen species, a flow of ethane was switched to one of helium, and a TPD was carried out to 1073 K. Carbon dioxide was sluggishly desorbed above 1023 K. This suggested that deep oxidation of ethane occurred along with the oxidative dehydrogenation of ethane in the course of TPRx with adsorbed oxygen species. However, because the desorption occurred at a very slow rate, the total amount of carbon dioxide desorbed was difficult to estimate under the present experimental conditions. On the as-

sumption that the stoichiometry of the oxidative dehydrogenation with adsorbed oxygen species was represented by that with gaseous oxygen as  $\text{C}_2\text{H}_6 + \frac{1}{2}\text{O}_2 \rightarrow \text{C}_2\text{H}_4 + \text{H}_2\text{O}$ , the amount of adsorbed oxygen species consumed for this reaction was determined on the basis of that of ethene estimated from the peak areas of  $\alpha$ - and  $\beta$ -peaks. Over the catalyst having  $0.013 \mu\text{mol}/\text{m}^2\text{CaO}$  of adsorbed oxygen species, the oxygen species consumed amounted to  $0.0094 \mu\text{mol}/\text{m}^2\text{CaO}$ . From these values, the selectivity was estimated to be 72% for the oxidative dehydrogenation of ethane with adsorbed oxygen species. With increasing the amount of adsorbed oxygen species present on the surface, the selectivity decreased appreciably. Over the catalyst with  $0.37 \mu\text{mol}/\text{m}^2\text{CaO}$  of adsorbed oxygen species, the selectivity dropped to 31%. Hence, we concluded that the oxidative dehydrogenation of ethane occurred with high selectivity with oxygen species located at the sites with a coordination number of 4.

#### REFERENCES

1. Seiyama, T., "Metal Oxides and Their Catalytic Functions." Kodansha Scientific Co., Tokyo, 1978. [In Japanese].
2. Nelson, R. J., Tench, A. J., and Harmworth, B. J., *Trans. Faraday Soc.* **63**, 1427 (1967).
3. Nelson, R. L., and Tench, A. J., *Trans. Faraday Soc.* **63**, 3039 (1967).
4. Lunsford, J. H., and Jayne, J. P., *J. Chem. Phys.* **44**, 1487 (1966).
5. Derouane, E. G., and Indovina, V., *Chem. Phys. Lett.* **14**, 455 (1972).
6. Ito, T., Kato, M., Toi, K., Shirakawa, T., Ikemoto, I. and Tokuda, T., *J. Chem. Soc. Faraday Trans. 1* **81**, 2835 (1985).
7. Tashiro, T., Ito, T. and Toi, K., *J. Chem. Soc. Faraday Trans. 1* **86**, 1139 (1990).
8. Nakamura, M., Mitsuhashi, H., and Takezawa, N., *React. Kinet. Catal. Lett.*, in press.
9. Garrone, E., Zecchina, A., and Stone, F. S., *Philos. Mag.* **42**, 683 (1980).
10. Collucia, S., Deane, A. M., and Tench, A. J., *J. Chem. Soc. Faraday Trans. 1* **74**, 2913 (1978).
11. Zecchina, A., Lofthouse, M. G., and Stone, F. S., *J. Chem. Soc. Faraday Trans. 1* **71**, 1476 (1975).
12. Levine, J. D., and Mark, P., *Phys. Rev.* **144**, 751 (1966).
13. Collucia, S., and Tench, A. J., in "Proceedings, 7th

- International Congress on Catalysis'' (T. Seiyama and K. Tanabe, Eds.), Vol. B, p. 1154. Elsevier, New York, 1981.
14. Matsukata, M., Okanari, E., Kobayashi, K., Kikuchi, E., and Morita, Y., *Shokubai [Catalyst]* **30**, 400 (1988).
15. Nakamura, M., Fujita, S., and Takezawa, N., *Catal. Lett.*, in press.
16. Ito, T., Yoshioka, M., and Tokuda, T., *J. Chem. Soc. Faraday Trans. 1* **79**, 2277 (1983).
17. Indovina, V., and Cordischi, D., *J. Chem. Soc. Faraday Trans. 1* **78**, 1705 (1982).